Reprinted from the Journal of The American Ceramic Society, Vol. 62, No. 7–8 July–August, 1979

Contact-Induced Failure of Prestressed Glass Plates

P. CHANTIKUL, B. R. LAWN,* and D. B. MARSHALL

Department of Applied Physics, School of Physics, University of New South Wales, Kensington, New South Wales 2033, Australia

An indentation fracture technique was used to determine critical contact conditions under which prestressed brittle surfaces are subject to catastrophic failure. A theoretical model based on the growth of a well-developed, contact-induced half-penny crack leads to a simple inverse-cube power relation between indentation load and tensile prestress. The analysis is developed in terms of fracture parameters which are readily calibrated in routine indentation/strength tests. Experiments on glass disks loaded simultaneously in biaxial flexure and Vickers indentation confirm the essential failure predictions of the theory; toughness is the key material parameter controlling resistance to failure. The results emphasize the danger of spurious tensile stresses in ceramic systems exposed to severe contact events.

I. Introduction

BRITTLE surfaces can suffer serious cracking in contact situations, particularly in impact with sharp solid particles. Much attention has been devoted to one particular aspect of this problem, viz. that of strength degradation where the surface is first indented and then stressed to failure.[1–8] The question of failure during indentation, on the other hand, has been largely overlooked. Yet this second situation is potentially as dangerous as the first: indentation cracks, although usually highly stable, can in unfavorable circumstances become prematurely unstable. Thin plates impacted with heavy projectiles, in which contact-induced cracks experience flexural stresses on rebound,[9] and tempered plates, where the cracks penetrate into an inner tension region,[10] are pertinent examples of catastrophic failure situations.

In the present study an analysis is given of surfaces prestressed in tension and exposed to severe contact events. Earlier investigations by Kirchner and Gruver[11–13] into the nature and extent of the damage incurred by flexure-loaded glass and ceramic plates during impact with small spheres foreshadow the approach adopted here. Indentation fracture mechanics is used to determine the critical combination of surface tensile stress and contact load at which failure occurs. Experiments on a model system involving glass disks with their prospective contact surfaces in biaxial tension and a statically loaded Vickers pyramid indenter confirm the essential theoretical predictions. The critical contact load to failure is extremely sensitive to the preexisting stress level, a result pertinent to the design of engineering ceramics.

II. Prediction of Failure Conditions

Suppose that a brittle surface is exposed to some contact event, such that the load delivered is sufficient to produce a dominant, well-developed penny-like flaw configuration.[14] Consideration may then be given to the potential failure of the system from this flaw under the action of a tensile stress, applied either after or during the contact process. Intuitively, it might be expected that the second of these two possible stress situations should be more deleterious,

Received June 26, 1978; revised copy received October 26, 1978.

Supported by the Australian Research Grants Committee. P. Chantikul's work was supported in part by a Commonwealth Government Grant under the Colombo Plan.

*Member, the American Ceramic Society.

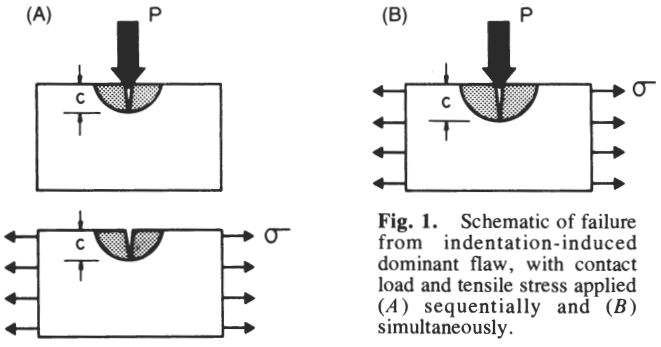

Fig. 1. Schematic of failure from indentation-induced dominant flaw, with contact load and tensile stress applied (*A*) sequentially and (*B*) simultaneously.

since the driving force on the indentation crack must be greater when the contributions from the contact load and tensile stress mutually reinforce each other.

Figure 1 illustrates the two cases; P is the indentation load, σ the applied tension at the contact surface, and c a characteristic crack dimension. The driving forces P and σ are applied sequentially in Fig. 1(*A*) and simultaneously in Fig. 1(*B*). A standard fracture mechanics analysis may be conducted for each of the cases presented, using the additive properties of stress-intensity factors.[15] Thus the stress-intensity factor for the indentation force system may be written[14]

$$K_P = \chi P/c^{3/2} \tag{1}$$

and for the applied tension force system as[15]

$$K_\sigma = \sigma(\pi\Omega c)^{1/2} \tag{2}$$

where χ and Ω are geometrical, dimensionless constants. In a complete analysis attention must be paid to several factors which influence these geometrical constants.[5] For example, Eq. (1) is derived in the context of ideally elastic loading at the penny center, but, in reality, elastic/plastic "mismatch" stresses associated with the inelastic deformation which inevitably surrounds the sharp-contact point can profoundly influence the effective value of χ; again, the presence of free surfaces and stress gradients in the applied stress system will reflect in Ω. However, with an expedient choice of experimental procedure most of these complications can be neglected in the present analysis.

The situation of primary interest here is that of Fig. 1(*B*). The crack is assumed to grow under conditions of equilibrium, $K = K_c$,[15] so that

$$K_P + K_\sigma = K_c \tag{3}$$

Combining Eqs. (1), (2), and (3) then gives expressions for either the load P or stress σ in terms of the crack size c:

$$P = (K_c c^{3/2}/\chi)[1 - \sigma(\pi\Omega c)^{1/2}/K_c] \tag{4a}$$

$$\sigma = [K_c/(\pi\Omega c)^{1/2}](1 - \chi P/K_c c^{3/2}) \tag{4b}$$

These functions are plotted schematically in Fig. 2. The growth of the crack is stable up to a critical size c^*, beyond which instability sets in. The requirement for failure is therefore that a maximum P^* or σ^* be reached in the respective curves, i.e. that $(\partial P/\partial c)_\sigma$ or $(\partial\sigma/\partial c)_P$ be zero. From Eq. (4) this requirement reduces to

$$(\sigma^3 P^*)_\sigma = (\sigma^{*3} P)_P = (\sigma^3 P)^* = 27K_c^4/256\chi(\pi\Omega)^{3/2} \tag{5}$$

at which point

$$c^* = (4\chi P^*/K_c)^{2/3} = 9K_c^2/16\pi\Omega\sigma^{*2} \tag{6}$$

Note that the conditions represented by Eqs. (5) and (6) are independent of the loading path, e.g. by increasing P at constant σ or vice versa.

Thus, given values of K_c, χ, and Ω, the appropriate failure conditions may be predicted a priori for any brittle surface subjected to simultaneous tensile stress and contact loading. However, these parameters are not always readily available. In particular, K_c generally must be determined from some independent crack-propagation test.[16] This difficulty, along with those discussed previously in

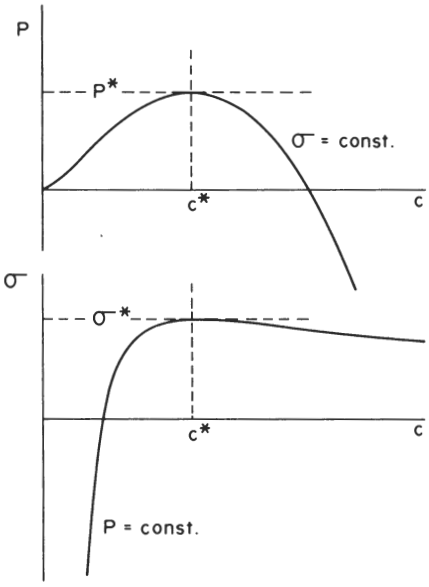

Fig. 2. Plot of functions in Eq. (4); critical configuration is denoted by asterisk notation.

connection with the values of χ and Ω, can be conveniently circumvented by investigating the fracture mechanics of the indentation-force and applied-tension systems in mutual isolation. Then from Eq. (1) the appropriate (stable) equilibrium relation is

$$(P/c^{3/2})_{\sigma=0} = K_c/\chi = \text{constant} \tag{7}$$

and likewise from Eq. (2) the (unstable) equilibrium relation is

$$(\sigma c^{1/2})_{P=0} = K_c/(\pi\Omega)^{1/2} = \text{constant} \tag{8}$$

Then, if suitable precautions are taken to ensure that the geometrical conditions governing the terms χ and Ω in Eqs. (7) and (8) are essentially equivalent to those in Eq. (4), simple "calibration constants" may be obtained for insertion into the failure equation, and Eq. (5) may be restated in the form

$$(\sigma^3 P)^* = (27/256)\,(\sigma c^{1/2})_{P=0}{}^3 (P/c^{3/2})_{\sigma=0} \tag{9}$$

III. Experimental Results

(1) Test Procedure

The specimens used to test the preceding analysis were soda-lime glass disks, nominally 50 mm in diam. by 3 mm thick, which could be put into any specified level of biaxial surface tensile stress using a coaxial ring assembly (Fig. 3). The rings were driven by hydraulic

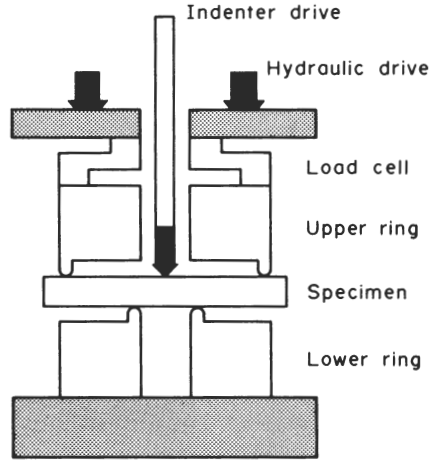

Fig. 3. Experimental arrangement for stressing contact-loaded plates to failure.

pressure and a load cell was used to record the driving force. Standard formulas for thin plates in flexure[17] were used to evaluate the tensile stress at the contact site; the evaluation included a correction term to allow for a small component of surface compression introduced by the indentation loading.

The indentation load itself was delivered under dead-weight conditions on a conventional hardness-testing machine, using a Vickers diamond pyramid indenter. In most normal glass surfaces the Vickers pyramid initiates half-penny "median" cracks on mutually orthogonal planes containing the load axis and one of the indentation diagonals.[14,18] (Other cracks are also produced, but they are not pertinent to strength considerations.) The assembly of Fig. 3 could be mounted onto the base plate of the hardness tester and the stressed surfaces of the glass disks indented in situ. The axial symmetry of the applied stress field eliminated any need to orient the indentations.

In all tests the contact site was maintained free of moisture, either by covering it with a drop of paraffin oil or by enclosing the specimen assembly within a dry N_2 gas stream. This procedure eliminated the complication of chemical kinetic effects.

(2) Calibration Parameters for Failure Prediction

In applying the analysis of Section II to the evaluation of prospective contact-induced failure in tensile-stressed plates, appropriate parameters must first be determined for Eqs. (5) or (9). The approach taken here is via the second of these equations, using calibration tests to specify the constants in Eqs. (7) and (8).

For the constant in Eq. (7), indentation tests were conducted with the glass disks placed on a flat base to ensure zero surface stress. The sizes of the median cracks were measured from residual surface traces, on the basis of near-ideal half-penny geometry.[5,14] These measurements, made on some 40 indentations at loads of 2 to 100 N, gave

$$(P/c^{3/2})_{\sigma=0} = (10.1 \pm 0.5) \text{ MPa m}^{1/2} \quad (10)$$

For the constant in Eq. (8), strength was measured on disks containing well-defined indentation half-penny cracks. However, examination of the indentation sites in polarized light prior to rupture in the strength test showed evidence of substantial residual elastic/plastic stresses. Although the effects of such stresses are automatically incorporated in the χ term of Eq. (7),[5] the validity of Eq. (8) rests on the applied tension being the only driving force on the cracks. The indented disks were accordingly annealed until all traces of the residual stress field were removed. In case this procedure had caused any crack-tip blunting, the disks were then stressed subcritically in tension in a moist environment until some slow crack growth was observed. The test environment was then restored to that of dry N_2, the surface traces of the median cracks measured, and the plates stressed to failure. Results from 20 plates in the fracture-stress range 35 to 70 MPa gave

$$(\sigma c^{1/2})_{P=0} = (0.77 \pm 0.05) \text{ MPa m}^{1/2} \quad (11)$$

Inserting these two calibration constants into Eq. (9) then gives the failure condition

$$(\sigma P^{1/3})^* = (79 \pm 7) \text{ MPa N}^{1/3} \quad (12)$$

(3) Contact-Induced Failure Tests

Seventy plates were taken to failure using the combined indentation/stress system of Fig. 3. For practical purposes the indenter was loaded onto the test surface before applying the flexural stress; the dead-weight loading of the indentation then provided a convenient route to the critical configuration via the condition $(\partial\sigma/\partial c)_P = 0$. It was noted during preliminary tests that the threshold for median crack formation was not always exceeded during indenter loading, but rather during unloading: in the interest of a "worst-case" analysis, therefore, a load/unload/reload indentation sequence was adopted.

The results are plotted in Fig. 4. The predicted and observed failure characteristics differ slightly, even allowing for scatter bands. Conveniently, the predictions underestimate the failure stress, as required by conservative design. At low indentation loads σ^* becomes greater than the strength of the as-received surfaces,

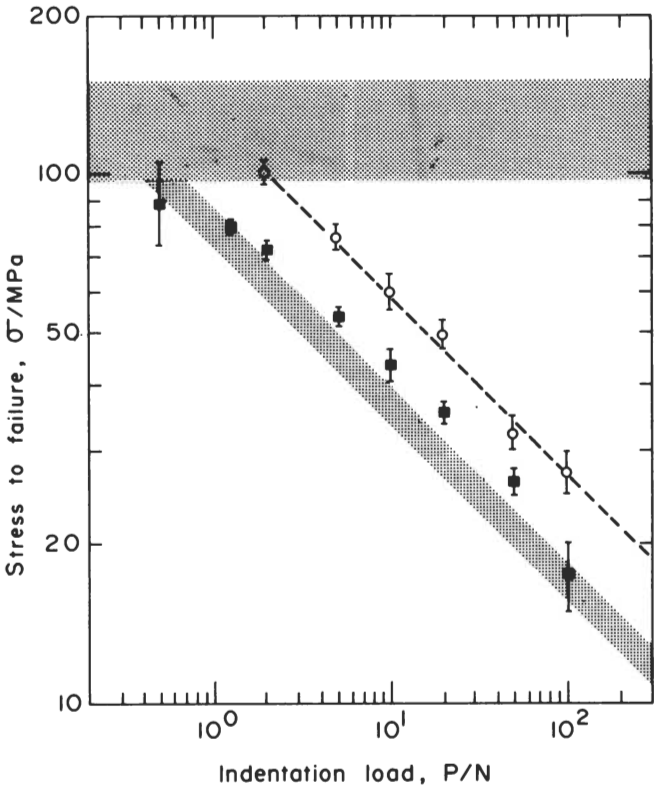

Fig. 4. Failure stress as function of contact load, for Vickers indentations on soda-lime glass disks. Each data point represents mean and standard deviation of 8 to 10 tests. Filled symbols are measured critical conditions (σ^*, P^*) in loading configuration of Fig. 1(*B*); inclined shaded band is corresponding prediction of Eq. (9). Open symbols are comparative strength degradation data in loading configuration of Fig. 1(*A*); broken line is curve fit to these data. Horizontal shaded band designates cutoff strength level for the as-received surfaces.

$>(123 \pm 25)$ MPa (20 plates); i.e. at $P << 1$ N the surface stresses produce critical cracks smaller than typical preexistent flaws and are relatively innocuous. At high indentation loads, however, σ^* decreases very rapidly and the stress state becomes highly dangerous.

For comparison, data are included in Fig. 4 from tests in which the surface stressing was applied after, rather than during, the indentation, i.e. using the configuration of Fig. 1(*A*) rather than Fig. 1(*B*). As expected, since the indentation and applied-tension force systems do not mutually enhance each other in this configuration, these data points lie above those obtained in combined loading.

IV. Discussion

The fracture mechanics analysis presented here provides a useful basis for characterizing the prospective integrity of brittle components in combined indentation/surface-stress situations. Thus, given a candidate ceramic material for any structural application in which some in-service contact event is likely to produce a dominant flaw, failure conditions may be predicted from simple calibration tests in the laboratory. The present treatment of a specific model system in the test program does not detract from the generality of the analysis; it is, for instance, a straightforward matter to relate calibration data obtained with a statically loaded pyramid indenter to an impact situation involving irregular sharp particles.[7,8]

Equation (5) shows that toughness, K_c, is the controlling material parameter in failure resistance: at constant contact load $\sigma^* \propto K_c^{4/3}$ and at constant tensile prestress $P^* \propto K_c^4$. As in most other strength considerations,[6] the primary design aim must be to maximize this parameter. The other factor usually involved in strength discussions, preexistent flaw size, assumes an insignificant role in the formulation; the contact event initiates its own critical crack, so flaw statistics influence nothing more than the "cutoff" strength level at

low indentation loads (Fig. 4). Accordingly, other than in their indirect influence on K_c, or in their possible introduction of residual surface compressive stresses,[5,6] surface and microstructural refinements do not afford a practical route to increased failure resistance.

The results of Eqs. (5) and (9) show that the critical contact load to fracture is highly sensitive to the level of prestress. For example, consider a circular plate subjected to a uniform pressure difference of 1 atm across its faces. If the plate is freely supported at its edge, a maximum tensile stress of $\approx(a/t)^2$ atmospheres develops at the center of the low-pressure face, where a/t is the ratio of disk radius to thickness.[17] Taking atmospheric pressure as ≈ 0.1 MPa and a typical ratio $a/t \approx 15$ gives a maximum tension of ≈ 20 MPa. Now suppose that the tensile region of the plate is subjected to a contact event. According to Fig. 4, a load $P^* \approx 100$ N would be sufficient to take the plate to failure. Such a load would be achieved, for instance, in an impact at 100 m s^{-1} by a sharp particle of mass ≈ 0.2 mg (e.g. by a quartz particle ≈ 500 μm in diam.).[7] It is clear that design specifications must include safeguards against the occurrence of spurious tensile stresses in any vital brittle component exposed to solid particle contact.

The failure equations should not be applied to any particular system without due consideration to certain simplifying assumptions in the analysis. Among these assumptions are those mentioned in connection with the constants χ and Ω in Eqs. (1) and (2). For instance, it was indicated that stress gradients over the crack area can influence the second of these constants. Since the contact surface is stressed via a flexure mode in the experimental setup of Fig. 3, such effects could become important if the critical crack size were not to remain small in comparison with the plate thickness. Taking $K_c \approx 0.8$ MPa $m^{1/2}$ for glass[19] and $\Omega \approx 4/\pi^2$ for ideal penny cracks,[3] a maximum crack size corresponding to the minimum stress level $\sigma^* \approx 17$ MPa recorded in Fig. 4 is calculated from Eq. (6) at $c^* \approx 1$ mm, i.e. about one-third the plate thickness. Again, the potential effects of residual stresses associated with elastic/plastic mismatch about the deformation zone have been neglected. Such difficulties tend to be obscured in the "calibration" procedure leading to Eq. (9), where both χ and Ω are eliminated from the formulation. The physical significance of these parameters, together with some important implications in certain facets of the strength-degradation problem, will be considered in greater detail elsewhere.[20,21]

Acknowledgment: The writers thank H. P. Kirchner for discussions which provided the stimulation for the present study.

References

[1] A. G. Evans, "Strength Degradation by Projectile Impacts," *J. Am. Ceram. Soc.*, **56** [8] 405–409 (1973).
[2] B. R. Lawn, S. M. Wiederhorn, and H. H. Johnson, "Strength Degradation of Brittle Surfaces: Blunt Indenters," *ibid.*, **58** [9–10] 428–32 (1975).
[3] B. R. Lawn, E. R. Fuller, and S. M. Wiederhorn, "Strength Degradation of Brittle Surfaces: Sharp Indenters," *ibid.*, **59** [5–6] 193–97 (1976).
[4] S. M. Wiederhorn and B. R. Lawn, "Strength Degradation of Glass Resulting from Impact with Spheres," *ibid.*, **60** [9–10] 451–58 (1977).
[5] D. B. Marshall and B. R. Lawn, "Strength Degradation of Thermally Tempered Glass Plates," *ibid.*, **61** [1–2] 21–27 (1978).
[6] B. R. Lawn and D. B. Marshall; pp. 205–29 in Fracture Mechanics of Ceramics, Vol. 3. Edited by R. C. Bradt, D. P. H. Hasselman, and F. F. Lange. Plenum, New York, 1978.
[7] S. M. Wiederhorn and B. R. Lawn, "Strength Degradation of Glass Impacted with Sharp Particles: I," *J. Am. Ceram. Soc.*, **62** [1–2] 66–70 (1979).
[8] B. R. Lawn, D. B. Marshall, and S. M. Wiederhorn, "Strength Degradation of Glass Impacted with Sharp Particles: II," *ibid.*, pp. 71–74.
[9] J. L. Galthart and F. W. Preston, "The Behavior of Glass Under Impact: Theoretical Considerations," *Glass Technol.*, **9** [4] 89–100 (1968).
[10] B. R. Lawn and D. B. Marshall, "Contact Fracture Resistance of Physically and Chemically Tempered Glass Plates: A Theoretical Model," *Phys. Chem. Glasses*, **18** [1] 7–18 (1977).
[11] H. P. Kirchner and R. M. Gruver, "Localized Impact Damage in Stressed Members," *Mater. Sci. Eng.*, **28** [2] 249–55 (1977).
[12] H. P. Kirchner, "Analysis of Localized Impact Damage in Biaxially Stressed Glass Plates," *J. Am. Ceram. Soc.*, **61** [3–4] 161–63 (1978).
[13] H. P. Kirchner and R. M. Gruver, "Localized Impact Damage in Stressed Al_2O_3 and Si_3N_4," *Mater. Sci. Eng.*, **34** [1] 25–31 (1978).
[14] B. R. Lawn and E. R. Fuller, "Equilibrium Penny-Like Cracks in Indentation Fracture," *J. Mater. Sci.*, **10** [12] 2016–24 (1975).
[15] B. R. Lawn and T. R. Wilshaw, Fracture of Brittle Solids; Ch. 3. Cambridge University Press, London, 1975.
[16] A. G. Evans; pp. 17–48 in Fracture Mechanics of Ceramics, Vol. 1. Edited by R. C. Bradt, D. P. H. Hasselman, and F. F. Lange. Plenum, New York, 1974.
[17] R. J. Roark, Formulas for Stress and Strain, 4th ed.; Ch. 10. McGraw-Hill, New York and London, 1965.
[18] B. R. Lawn and M. V. Swain, "Microfracture Beneath Point Indentations in Brittle Solids," *J. Mater. Sci.*, **10** [1] 113–22 (1975).
[19] S. M. Wiederhorn, "Fracture Surface Energy of Glass," *J. Am. Ceram. Soc.*, **52** [2] 99–105 (1969).
[20] D. B. Marshall and B. R. Lawn, "Residual Stress Effects in Sharp-Contact Cracking: I"; to be published in *Journal of Materials Science*.
[21] D. B. Marshall, B. R. Lawn, and P. Chantikul, "Residual Stress Effects in Sharp-Contact Cracking: II"; to be published in *Journal of Materials Science*.